Experimental Evidence for Hydrophobic Matching and Membrane-Mediated Interactions in Lipid Bilayers Containing Gramicidin

Thad A. Harroun, William T. Heller, Thomas M. Weiss, Lin Yang, and Huey W. Huang
Physics Department, Rice University, Houston, Texas 77251 USA

ABSTRACT Hydrophobic matching, in which transmembrane proteins cause the surrounding lipid bilayer to adjust its hydrocarbon thickness to match the length of the hydrophobic surface of the protein, is a commonly accepted idea in membrane biophysics. To test this idea, gramicidin (gD) was embedded in 1,2-dilauroyl-*sn*-glycero-3-phosphocholine (DLPC) and 1,2-myristoyl-*sn*-glycero-3-phosphocholine (DMPC) bilayers at the peptide/lipid molar ratio of 1:10. Circular dichroism (CD) was measured to ensure that the gramicidin was in the $\beta^{6.3}$ helix form. The bilayer thickness (the phosphate-to-phosphate distance, or PtP) was measured by x-ray lamellar diffraction. In the L_α phase near full hydration, PtP is 30.8 Å for pure DLPC, 32.1 Å for the DLPC/gD mixture, 35.3 Å for pure DMPC, and 32.7 Å for the DMPC/gD mixture. Gramicidin apparently stretches DLPC and thins DMPC toward a common thickness as expected by hydrophobic matching. Concurrently, gramicidin-gramicidin correlations were measured by x-ray in-plane scattering. In the fluid phase, the gramicidin-gramicidin nearest-neighbor separation is 26.8 Å in DLPC, but shortens to 23.3 Å in DMPC. These experiments confirm the conjecture that when proteins are embedded in a membrane, hydrophobic matching creates a strain field in the lipid bilayer that in turn gives rise to a membrane-mediated attractive potential between proteins.

INTRODUCTION

Some membrane proteins bind lipid molecules stereospecifically, as in the case of bactericidal/permeability-increasing protein (Beamer et al., 1997). Others interact nonspecifically with a lipid bilayer as a bulk material, as in the case of rhodopsin (Brown, 1997). The second type of interaction is interesting because there is a great disparity in the elastic constants between proteins and lipid bilayers. Lipid bilayers are very deformable because of the flexibility of the lipids' hydrocarbon chains. For example, the thickness compressibility of dimyristoylphosphatidylcholine (DMPC) in the fluid phase is $\sim 2 \times 10^{-9}$ cm^2/dyn. (The rate of thickness change by pressure normal to the bilayer is estimated from the area stretchability measured by Evans and Needham, 1987.) However, globular proteins are more rigid. A deformation of a globular protein often involves changes of bond lengths. One may roughly estimate protein deformability by its volume compressibility, which is $\sim 5 \times 10^{-12}$ cm^2/dyn for lysozyme or ribonuclease A (Gekko and Noguchi, 1979). In this sense, membranes are 400 times more deformable than proteins. Therefore, when a protein is embedded in a lipid bilayer, one expects the lipid bilayer surrounding the protein to adjust its hydrocarbon thickness to match the length of the hydrophobic surface of the protein. This idea of hydrophobic matching assumes the energy of the membrane deformation is less than the energy cost of hydrophobic mismatch; that is, if the matching were not to occur. The latter can be estimated by the free energy increase for transferring a hydrophobic protein surface from an organic solvent to an aqueous environment, which is ~ 17 erg/cm^2 (Chothia, 1974). Although the concept of hydrophobic matching has been around for a long time (see an early review by Abney and Owicki, 1985), so far there has not been a direct measurement to support the conjecture.

A possible consequence of the membrane deformation is membrane-mediated interactions between proteins (Marcelja, 1976; Schroeder, 1977; Owicki and McConnell, 1979). Such interactions are likely long-ranged (over many lipid molecules) and may be responsible for inhomogeneous lateral distributions of intrinsic membrane proteins, and consequently the functional specialization of regions in biological membranes (Stoeckenius et al., 1979; Loewenstein, 1981; Lewis and Engelman, 1983; Abney and Owicki, 1985). The first experimental investigations on this problem using artificial membranes were done by Lewis and Engelman (1983) and Pearson et al. (1983). The distribution of bacteriorhodopsin (BR) and rhodopsin (RH) in lipid bilayers of various thicknesses were examined by freeze-fracture electron microscopy (EM). Some correlations between the bilayer thickness and the protein distribution were observed. For BR in di 12:0, di 14:0, and di 16:0 phosphatidylcholines (PC) bilayers, EM pictures revealed no evidence for interactions between particles other than those resulting from the hard core repulsion. Only in very thin di 10:0 and very thick di 24:1 PC bilayers was BR aggregation observed. Bleached RH in di 12:0 PC and di 18:1 trans-PC and dark-adapted RH in di 10:0 PC showed evidence of an additional repulsive interaction at long range, but for dark-adapted RH in di 18:1 trans-PC there appeared to be an additional attractive interaction which was proposed to be membrane-mediated. The interpretation of these results was not straightforward. BR and RH are complex enough that the properties of the protein-lipid boundaries are unknown. Protein denaturation and bleaching-induced molecular charge were cited as pos-

Received for publication 6 May 1998 and in final form 30 September 1998.
Address reprint requests to Dr. Huey W. Huang, Physics Department, Rice University, Houston, TX 77251-1892. Tel.: 713-527-4899; Fax: 713-527-9033; E-mail: huang@ion.rice.edu.

0006-3495/99/02/937/09 $2.00

sible complications (Pearson et al., 1983). Finally, the possibility that the freezing process altered the protein distribution in bilayers could not be excluded (Pearson et al., 1984). Since this pioneering work, no other systematic experimental studies of this problem were published in the literature, despite a great deal of theoretical interest (see reviews by Abney and Owicki, 1985 and by Goulian, 1996). In this and a following paper we measure and analyze the problems of hydrophobic matching and membrane-mediated interaction with a simple, well-defined protein-lipid system. We study gramicidin distributions in di 12:0 PC (DLPC) and di 14:0 PC (DMPC) bilayers with x-ray diffraction. The protein correlations in the plane of the membrane were measured by in-plane scattering, and concurrently the average bilayer thickness was measured by lamellar diffraction.

Gramicidin, a 15-amino acid peptide, forms a well-defined dimeric channel in lipid bilayers (Arseniev et al., 1985; Ketchem et al., 1993). The backbone of the channel is in a β-helix configuration because of its L-D alternating sequence, with largely hydrophobic side chains covering the exterior surface. Two monomers are joined by six hydrogen bonds formyl end-to-formyl end to form the dimeric channel. The conformation of gramicidin in lipid bilayers can be examined by circular dichroism (CD). We also have some understanding about the channel-lipid interaction. In particular, the effect of bilayer thickness on the channel lifetime (Elliott et al., 1983) has been explained by a channel-induced membrane deformation energy (Huang, 1986). Thus there is a theoretical basis for analyzing the effect of membrane thickness on the in-plane distribution of gramicidin channels.

In the last few years we have developed the techniques of membrane in-plane scattering with x-ray and neutron, which directly measure protein-protein correlation in the fluid state of membranes (He et al., 1993a; see Blasie and Worthington, 1969 for an early application of this technique). The scattering curve provides the information about the size and shape of the scattering objects, as well as their in-plane correlations (He et al., 1993b, 1994, 1995, 1996a). This is the most direct way of demonstrating membrane-mediated interactions between embedded proteins (Pearson et al., 1983). The method of measuring membrane thickness has also been refined recently (Wu et al., 1995; He et al., 1996b; Nagle et al., 1996; Chen et al., 1997). In this paper we will describe the experiment and in a following paper we will discuss the theoretical interpretation.

EXPERIMENTAL

Sample preparation

1,2-dilauroyl- and 1,2-myristoyl-*sn*-glycero-3-phosphocholine (DLPC, DMPC) were purchased from Avanti Polar Lipids (Alabaster, AL). Gramicidin D (gD) was purchased from Sigma Chemical Company (St. Louis, MO). gD is a mixture of the naturally occurring analogs valine gramicidin A (85%), B, and C, and small amounts of isoleucine gramicidin A, B, and C. A, B, C differ at position 11: Trp for A, Phe for B, Tyr for C. Thallium(I) acetate was bought from Aldrich Chemical Company (Milwaukee, WI). All chemicals were used without further purification.

Lipid and peptide were mixed in the molar ratio of 10:1. For the x-ray in-plane scattering experiment, thallium was added in the ratio of one ion per peptide monomer to enhance the x-ray contrast between gramicidin channel and lipid background. The sample configuration for all experimental techniques described in this paper is the same: uniformly aligned lipid multilayers, with incorporated gramicidin, laying in large monodomains upon a flat substrate. The only difference between the samples for different techniques is the substrates. Oriented circular dichroism (OCD) and x-ray lamellar diffraction measurements used quartz slides, while x-ray in-plane measurements used substrates of small, polished beryllium disks. Two different sample preparations were used in this experiment, chiefly because in-plane scattering requires a much larger amount of sample compared to OCD and lamellar diffraction. To prepare large quantities of hydrated lipid-gramicidin mixtures, they were first co-dissolved in chloroform. The solvent was blown away under a stream of dry nitrogen, and the result was dried under vacuum to remove residual solvent. Several milliliters of distilled water were added to the dried lipid/protein mix, and the thallium(I) acetate was added to the solution. After 20 min of sonication to ensure thorough mixing and the breakup of possible aggregates, the solution was quick-frozen in a dry ice-ethanol bath. The sample was then lyophilized for 48 h. The sample bottle containing the white, fluffy, lyophilized powder was placed in a closed container with distilled water. The bottle was left uncovered so that the sample could come into contact with the water vapor. DLPC samples were left this way at room temperature to hydrate for several days to a couple of weeks. DMPC samples, by virtue of their higher main transition temperature, were left in this manner in a 35°C oven. After a couple of days, the samples became a clear, sticky gel, ready for use. However, experience showed that samples that hydrated for longer periods (at least a week) were more fluid and easier to work with.

X-ray in-plane scattering samples began by thoroughly cleaning two beryllium disks with ethanol. Five to eight milligrams of the hydrated sample were applied to the center of one disk, and the other disk was placed on top to make a substrate-sample-substrate sandwich. With slight pressure and temperature annealing, it was possible to align the sample such that the average membrane plane lies parallel to the substrates (Huang and Olah, 1987). A small amount of sample that might have oozed out the sides was carefully removed. OCD samples were made in a similar fashion, using quartz substrates. Because gramicidin has four tryptophans per monomer, CD spectra can be severely distorted (by absorption) with too much material. Thus, OCD samples were compressed until they were very thin and gave a clean, undistorted signal down to 200-nm wavelength.

X-ray lamellar diffraction doesn't require nearly as much sample as in-plane scattering. In fact, there is a much simpler sample-making technique that requires very little sample, and yields good results (Ludtke et al., 1995). A small glass disk was cleaned in hot sulfuric acid and washed with ethanol and distilled water. No more than 1 mg of lipid and peptide, co-dissolved in chloroform, was deposited upon the disk, and the solvent was allowed to evaporate in air. The sample was redissolved once, using a solvent mixture (to be mentioned below), and slowly dried. The result uniformly coats the quartz disk with multilayers aligned with the substrate. Through much experience in our lab, we have arrived at the solvent mixture of chloroform/trifluoroethanol (3:1) as one of several preferred solvent systems that provides uniform evaporation. The sample was then placed under vacuum for several hours to remove residual solvent, and placed in a container in contact with distilled water vapor until use. OCD samples were also prepared in this manner, using only one quartz substrate, to verify that both sample preparations were truly equivalent.

Oriented circular dichroism

CD spectra were taken on a Jasco-500A spectropolarimeter in the wavelength range of 340–200 nm. The substrates of the OCD samples were oriented perpendicular to the incident light beam. Any artifacts resulting from linear dichroism or linear birefringence were eliminated by averaging over rotations about the beam axis every 30° (Wu et al., 1990). The sample

was enclosed in a box with quartz windows that contained a small amount of water. The spectra were independent of temperature from 25° to 35°C.

X-ray in-plane scattering

The sample/beryllium disk sandwich was transferred to an aluminum holder, which was placed into a sample chamber held in the x-ray beam such that the x-ray was incident normal to the beryllium substrates. The holder was detachable from the rest of the chamber for ease in changing samples with a minimum disruption to the experimental set-up. The temperature of the holder was controlled by a thermoelectric element powered by a feedback circuit in series with a solid-state temperature probe. In this fashion, the sample holder temperature could be maintained to ±0.5°C. Sample hydration was controlled via humidity in the sample chamber, which was managed by a heated water bath, and another feedback circuit in series with a solid state humidity sensor (Ludtke et al., 1995; Chen et al., 1997). The RH in the sample chamber could thus be controlled at a stable 95 ± 2%. Before taking data, samples were left to equilibrate in the chamber for several hours.

Data were taken on an Enraf Nonius 590 x-ray generator using a CuKα (λ = 1.54 Å) source, operating at 40 kV/35 mA, and recorded on Kodak Direct Exposure Film. An Enraf Nonius precession camera was adapted to be used simply as a film and sample holder, with its precession mechanism turned off. The sample-to-film distance was measured to be 177 ± 1 mm with powdered sucrose as a standard. Air scattering tends to be a problem with such a large sample-to-film distance; thus a beam stop was positioned to shorten the direct beam to diminish air scattering, but still allow detection of the small angle region. A sample of pure lipid was used as a measure of the background. Film exposure times lasted, on average, 4 h.

After the film was exposed, it was developed in Kodak GBX developer and fixer. To extract the data from the film, it was scanned into a computer on a standard flat-bed scanner with an attachment to record transparent media such as film. The scanner was calibrated to convert its measurement of grayscale to true optical density (Phillips and Phillips, 1985). Analysis software was written to find the center of the image and circularly integrate the powder pattern.

X-ray lamellar diffraction

The sample chamber for lamellar diffraction is similar to the in-plane chamber. The only difference is that the in-plane chamber is constructed for a transmission measurement, while the lamellar chamber is for reflection. Lamellar diffraction was collected on an Enraf Nonius Diffractus 581 and a Huber four-circle goniometer, with a line-focused (10 mm vertical × 1 mm horizontal) CuKα source operating at 40 kV and 15–30 mA. At a 6° take-off angle (the projected source dimension 10 × 0.1 mm^2) the incident beam was collimated by a horizontal soller slit and two vertical slits on the front and the back sides of the soller slit. The horizontal and vertical divergence of the incident beam were 0.23° and 0.4°, respectively. The diffracted beam first passed through a vertical slit and then was discriminated by a bent graphite monochromator before entering a scintillation detector that was biased to discriminate against higher harmonics. A diffracted beam monochromator has the advantage over an incident beam monochromator in that the Compton scattering and the fluorescence from the sample are screened; consequently the background signal is greatly reduced, which in turn allows the measurement of high diffraction orders.

One unique feature of membrane diffraction is that the repeat spacing is >30 times the x-ray wavelength. The momenta **q** satisfying the Bragg law lie very close to the surface of the Ewald sphere. As a consequence, it is very easy to obtain incorrect diffraction patterns with the sample misaligned in χ without realizing it (χ is the rotational angle around the line of intersection between the plane of scattering and the sample plane). We have established an elaborate routine for positioning and orienting lamellar samples, which was described in Wu et al. (1995).

After the sample alignment, the diffraction patterns were recorded by $\omega - 2\theta$ scan, repeated about every hour from $\omega = 0°$ to ~10°, with the step size $\Delta\omega = 0.02°$. For each temperature setting, the sample was scanned through a series of humidities ranging from RH ~98% to ~70%. For a given humidity setting, the hydration condition of the sample was considered to be in equilibrium if four consecutive scans produced the same pattern within a few percent. The four scans were then averaged to create one diffraction pattern for analysis.

RESULTS

Oriented circular dichroism

Fig. 1 shows the OCD data for gramicidin in aligned multilayers of DLPC and DMPC. The spectra could not be extended much below 210 nm because of strong UV absorbance of the gramicidin tryptophans. The spectra are very similar to published spectra of gramicidin in the dimeric channel state, including strong peaks around 217 and 236 nm, and a "ripple" around 290 nm (Huang and Olah, 1987).

X-ray lamellar diffraction

Typical diffraction patterns of pure DMPC and DMPC containing gramicidin are displayed in Fig. 2. In high humidities (RH > 98%), pure DMPC showed four or fewer Bragg orders because of damping by lamellar fluctuations (Caillé, 1972). As humidity decreased below 98%, the fluctuations diminished and the number of discernible Bragg orders rapidly increased to six or more. The pattern of six to eight orders persisted as the humidity decreased, until it reached a range of RH, different for different temperatures, in which the diffraction patterns showed two lamellar series, indicating that DMPC was undergoing the main transition from the L_α phase to a gel phase. The double series pattern turned into a single series again as we decreased the humidity further. DMPC in the gel phase showed 12 or more discernible Bragg orders.

In contrast, DMPC containing 1:10 (peptide/lipid) gramicidin exhibited no L_α-gel transition within the humidity

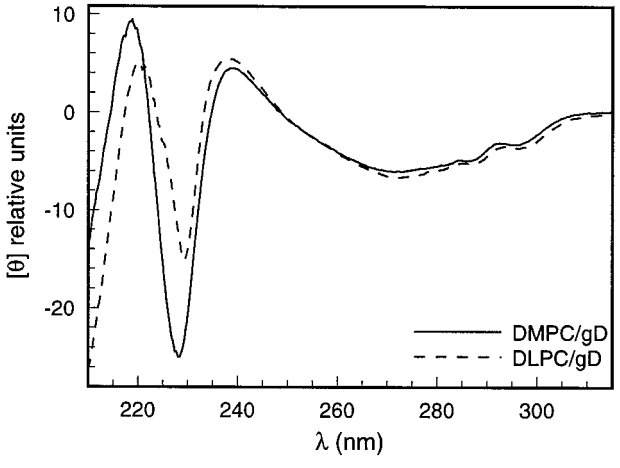

FIGURE 1 Oriented circular dichroism (OCD) of gramicidin embedded in DLPC and DMPC bilayers at the peptide to lipid molar ratio 1:10. The plane of membranes was oriented normal to the incident light beam.

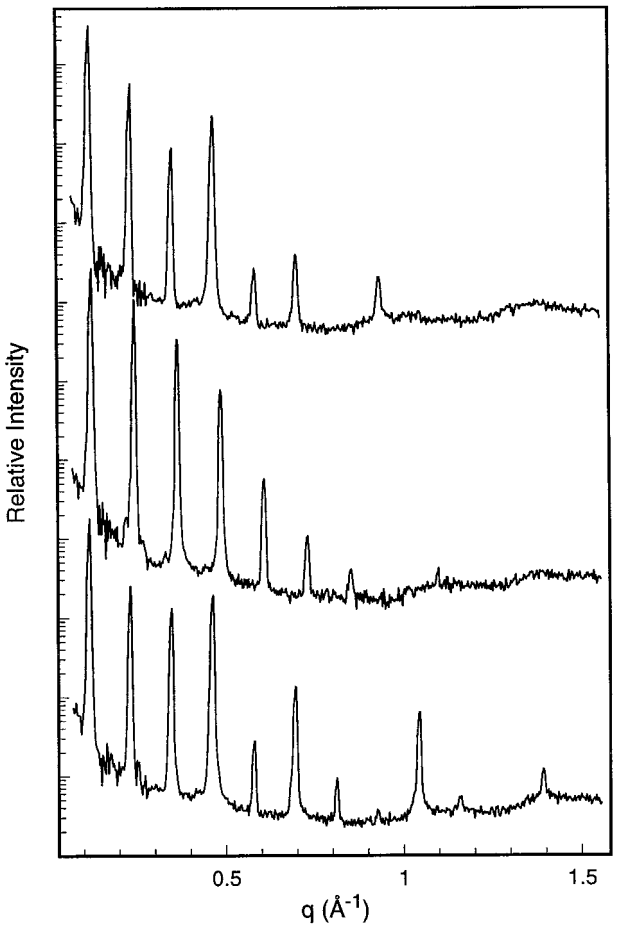

FIGURE 2 Typical x-ray diffraction patterns. *Top*: DMPC/gD (10:1) at 30°C, 96% RH. *Middle*: pure DMPC at 30°C, 96% RH. *Bottom*: DMPC at 30°C, 85% RH.

range of our experiment (~98% to ~70%). The diffraction patterns did not show damping or loss of Bragg orders in high humidities. The diffraction pattern consists of eight Bragg orders throughout the entire humidity range. This behavior is the same as DLPC containing the same ratio of gramicidin, reported previously in Olah et al. (1991).

We analyzed all diffraction patterns consisting of five or more discernible Bragg orders, in which the peaks are well defined, well separated, and do not show, within the resolution, noticeable broadening with Bragg order. The data reduction procedure has been described in detail in previous publications (Olah et al., 1991; Wu et al., 1995; He et al., 1996b; Chen et al., 1997). Briefly, it consists of the following steps. A background curve was generated by removing all of the Bragg peaks from all of the data sets of a particular sample, and then averaging the results and interpolating over any remaining gaps. After the background removal, a correction for the sample size versus the beam size, i.e., the diffraction volume, together with the absorption correction was carried out for each data point. Each Bragg peak was then fit with a Gaussian and integrated to obtain the intensity of that order. The integrated intensity was corrected for the polarization and the Lorentz factors. The square root of the integrated intensity is the relative magnitude of the scattering amplitude. The phasing diagrams were constructed by the Blaurock (1971) method (Fig. 3 *A*). With the phases determined, the relative scattering amplitudes were Fourier-transformed to produce unnormalized electron density profiles (Fig. 3 *B*), from which the peak-to-peak (PtP) distance was measured. PtP is unaffected by normalization of the electron density profile (Wu et al., 1995). Fig. 4 shows the PtP of DMPC with and without gramicidin at various temperatures as a function of the repeat spacing *d*. The PtP of DLPC has been published earlier (Olah et al., 1991; Chen et al., 1997).

X-ray in-plane scattering

Fig. 5 shows typical data for in-plane scattering. The inset shows the entire range of q that was collected, while the main frame focuses on the peak resulting from gramicidin. The raw data shown in the inset have the following features. The sharp strong peaks at $q \sim 0.12$ Å^{-1} are the first-order lamellar peaks because of the oily streak defects present in the multilayer samples. These smectic defects and their consequence on in-plane scattering have been discussed fully in previous papers (He et al., 1993a, 1996a). Note the absence of a second-order lamellar peak, except for a small one in DMPC/gD at 20°C (near $q = 0.24$ Å^{-1}), indicating

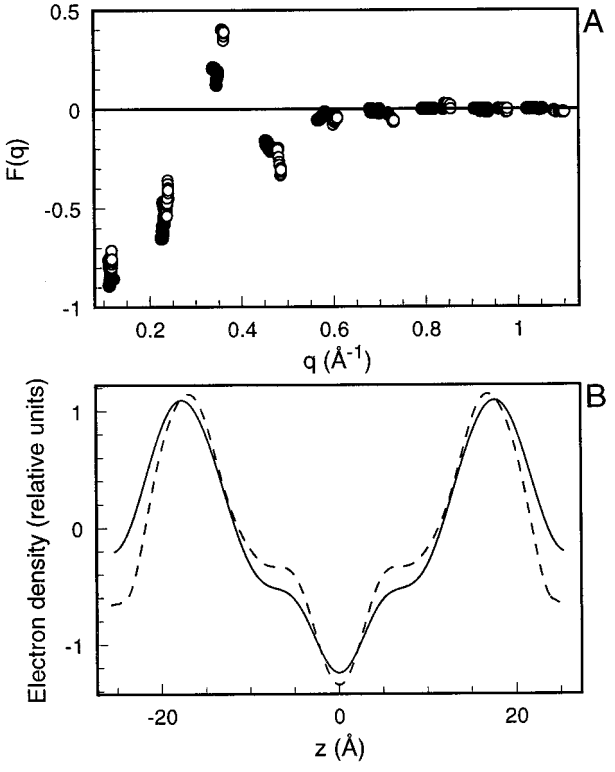

FIGURE 3 (*A*) Phasing diagrams for pure DMPC at 30°C (*open circles*) and DMPC/gD (10:1) at 30°C (*filled circles*). (*B*) Electron density profiles of pure DMPC at 30°C, 96% RH (*solid line*) and DMPC/gD (10:1) at 30°C, 94% RH (*dashed line*).

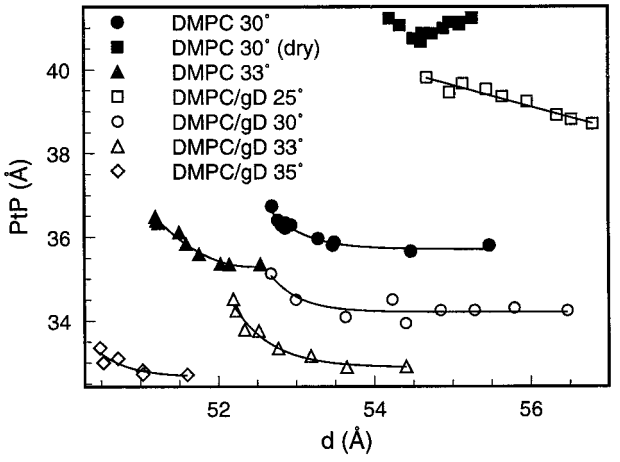

FIGURE 4 Peak-to-peak (PtP) distance of the electron density profile as a function of repeat spacing *d*.

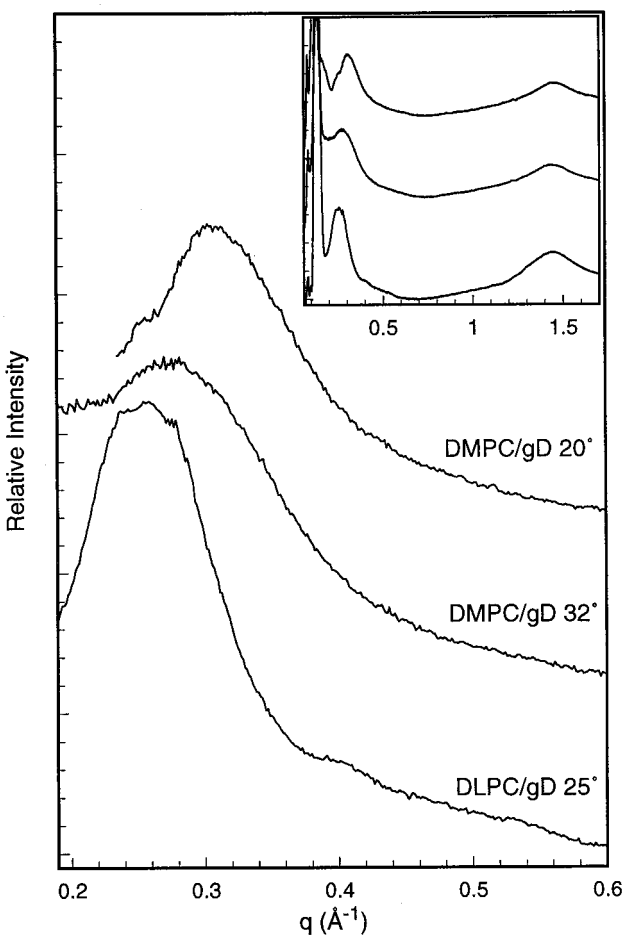

FIGURE 5 X-ray in-plane scattering curves. The inset shows the raw data of DMPC/gD (10:1) at 20°C, DMPC/gD (10:1) at 32°C, and DLPC/gD (10:1) at 25°C (*top* to *bottom*). The main frame shows the in-plane scattering curves after removing the background (pure lipid on the substrate). These are in-plane scattering curves of gramicidin.

that the samples were well aligned and contained only insignificant defects. The wide band near $q \sim 1.45$ Å^{-1} is the signal from lipid acyl chain packing, sometimes called the paraffin peak (Luzatti, 1968). The gramicidin correlation peak appears in the low angle beyond the defect peak, $q = 0.27$–0.33 Å^{-1}. Thallium ions have been added in the sample to enhance this peak. It is known that the gramicidin channel has high affinities for binding two thallium ions (Hinton et al., 1988). The great majority of the added thallium should be bound to the channels. Indeed, it was shown earlier that gramicidin without thallium produced the same in-plane scattering with a lower amplitude at the same correlation peak (He et al., 1993a). In-plane scattering from a pure lipid sample showed only the defect peak and the paraffin peak. The background signal composed of pure lipid and beryllium substrate was subtracted from the raw data to produce the three gramicidin curves in the main frame of Fig. 5. What is important in these data is that the gramicidin peak changes position as a function of lipid and temperature.

In Fig. 6 we recorded the position in q space of the scattering peak as a function of temperature. The open symbols are for DMPC and closed symbols for DLPC. The different symbols for DMPC are from different samples; note that they fall on the same curve. The peak position in DLPC is clearly independent of temperature. On the contrary, the peak position in DMPC shows a temperature-dependent transition. This corresponds to the gel-L_α transition observed by lamellar diffraction (see Fig. 4, DMPC/gD at 25°C vs. 30–35°C). The transition occurs between 27° and 31°C, ~5° higher than the normal main transition temperature (24°C) because of the sample being at ~95% RH, and the presence of gramicidin. Modification of lipid phase transition by gramicidin has been noted earlier at much lower peptide concentrations (Morrow and Davis, 1988).

DISCUSSION

Gramicidin is in the dimeric channel form

CD of gramicidin in the channel form was first identified by Urry et al. (1979a, b). The corresponding OCD was obtained by Huang and Olah (1987). In Fig. 1 gramicidin spectra in DLPC and DMPC show the characteristics of the previously identified channel form. However, identifying these spectra with the channel form could be misleading. We believe that these spectra reflect the $\beta^{6.3}$ helical configuration of gramicidin monomer (He et al., 1994). The CD spectra cannot distinguish a dimeric form from a monomeric form of gramicidin in $\beta^{6.3}$ helix. Nonetheless, we have reasons to believe that the samples used in our experiment are indeed in the dimeric channel form.

The first evidence is that similar sample preparations have been studied by NMR, which showed the peptide to be in the dimeric channel form (Ketchem et al., 1993; Koeppe et al., 1996). The second evidence is based on the measured association and dissociation constants of the dimer-mono-

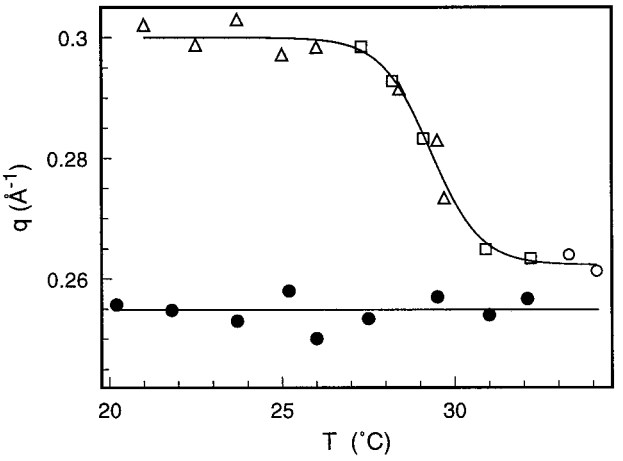

FIGURE 6 The peak position of gramicidin in-plane scattering in DMPC (*open symbols*) and in DLPC (*filled circles*) as a function of temperature. The peptide/lipid molar ratio is 1:10 in both. Different open symbols represent different DMPC samples. Note that they all fall on the same curve.

mer equilibrium in diphytanoylphosphatidylcholine (DPhPC) bilayers. According to Rokitskaya et al. (1996), the association constant is 4.6×10^{13} ($cm^2 \cdot s^{-1} \cdot mol^{-1}$) and the dissociation constant 0.48 s^{-1} at 26°C. At 1:10 peptide/lipid molar ratio, this implies that 2% of gramicidin is in the monomeric form. DMPC is thinner than DPhPC (Wu et al., 1995); therefore, dimers are favored in DMPC more than in DPhPC. We conclude that in both of our DMPC and DLPC samples >98% (most likely near 100%) of the gramicidin is in the dimeric channel form.

Hydrophobic matching

Thickness of fluid membrane has been measured in many different ways. Each method, though, has its own complications. For the diffraction method, the main problem is the bilayer's undulatory fluctuations (Caillé, 1972; Nagle et al., 1996), which damp out high Bragg orders and distort the remaining pattern. Our strategy for overcoming this difficulty consists of 1) obtaining high ordered diffraction patterns by dehydration that diminishes the fluctuations; 2) showing that the PtP is not affected by the remaining fluctuations; and 3) estimating the thickness (PtP) of fully hydrated membrane by extrapolation. This method has been demonstrated in detail (Wu et al., 1995; He et al., 1996b), including the particularly difficult region just above the main transition temperature (Chen et al., 1997), and is supported by the fluctuation analysis of Nagle et al. (1996).

The PtP distance should be very close to the phosphate-to-phosphate distance across the bilayer. That the peak position of the electron density profile corresponds to the position of the phosphate can be demonstrated by projecting the electron density of any reasonable lipid molecular model lengthwise (unpublished results). The electron density of a PC lipid is highest (40% higher than the average) at the phosphate group. The rest of the headgroup, i.e., phosphorylcholine minus PO_4, has an electron density close to that of water. Consequently the peak position, and hence the PtP, is relatively insensitive to the orientation of the phosphorylcholine relative to the plane of the bilayer.

It is well known that the main transition temperatures of diacylphophatidylcholines rise with dehydration (Smith et al., 1990; Chen et al., 1997). Therefore, at a temperature above the normal main transition (i.e., at full hydration), the lipid will undergo the L_α-gel transition in low humidities. One example, DMPC at 30°C, is shown in Fig. 4. In low humidities, the 30°C DMPC is in a gel phase with PtP ~41 Å. In high humidities, PtP is <37 Å, decreasing slowly as the humidity increases. As has been shown in many other examples (Wu et al., 1995; Ludtke et al., 1995; He et al., 1996b; Chen et al., 1997), in general PtP levels off as the repeat spacing *d* approaches the full hydration value. The PtP of pure DMPC decreases with temperature, but not significantly above 33°C (Chen, Hung, and Huang, in preparation). With 1:10 gramicidin, the main transition of DMPC is broadened and raised to a higher temperature. One example of the DMPC/gD mixture in the gel phase, at 25°C, is shown in Fig. 4. In the fluid phase, the PtP of DMPC/gD vs. *d* is similar to pure DMPC, except that it is thinner. The large drop in thickness from 30° to 33°C is because DMPC/gD is still in the gel-L_α transition region at 30°C. Above 35°C the PtP of the mixture is more or less of constant temperature.

In Table 1 we show the fluid phase PtP of DMPC and DLPC near 98% RH, with and without gramicidin. The thickness of pure DLPC was measured by Olah (1990) and independently by Chen et al. (1997) with the same result. DLPC/gD (10:1) was measured by Olah et al. (1991). It is important to point out that all these results were obtained by the same diffraction method and by the same data reduction procedure, so that even if there are systematic errors, the relative changes of the membrane thickness are still reliable. Pure DMPC is 4.5 Å thicker than pure DLPC, but when the lipids contain gramicidin in 10:1 ratio, the thicknesses of both of them approach a common value and become within 0.6 Å of each other. This is a strong indication of hydrophobic matching.

A recent paper by de Planque et al. (1998) describes using deuterium NMR to measure the effect of gramicidin on bilayer thickness. They reported thickening of DLPC, DMPC, and DPPC by gramicidin, in direct contradiction with our results. A possible explanation is in the use of the Seelig formula relating the thickness to the deuterium order parameter (Schindler and Seelig, 1975). The order parame-

TABLE 1 PtP of DLPC and DMPC at 98% RH

Bilayer	PtP	*T*
DLPC	30.8 Å	20°C
DLPC/gD (10:1)	32.1 Å	20°C
DMPC	35.3 Å	33°C
DMPC/gD (10:1)	32.7 Å	35°C

ter contains the average of $(\cos \alpha)^2$, where α is the angle between the bilayer normal and the deuterium bond vector CD, whereas the hydrocarbon thickness requires the average of $\cos \beta$, where β is the angle between the bilayer normal and the normal to the plane spanned by the two C–H bond vectors. It is impossible to obtain $\langle \cos \beta \rangle$ from $\langle (\cos \alpha)^2 \rangle$, unless the chains are restricted to a small number of possible configurations, as in the case of the Seelig formula, which was justified by a statistical model (Schindler and Seelig, 1975). However, even if the simple formula works for pure lipids, it may not be applicable to bilayers containing proteins.

Membrane-mediated interactions

For gramicidin channels embedded in a fluid bilayer or, in general, in a distribution without a long-range order, the 2D in-plane scattering intensity $I(q)$ is given by (He et al., 1993a; see also Blasie and Worthington, 1969).

$$\frac{I(q)}{I_e} = N|F(q)|^2 S(q), \tag{1}$$

where I_e is the scattering intensity by a single free electron; N is the number of channels; $F(q)$ is the scattering amplitude by an individual channel, called the form factor; $S(q)$ is the structure factor given by

$$S(q) = 1 + \iint [n(r) - \bar{n}] J_o(qr) 2\pi r \, dr \tag{2}$$

where $n(r)2\pi r dr$ is the average number of channels within the ring of radius r and width dr, centered at an arbitrarily chosen channel; $\bar{n}$ is the mean number density of channels; and $J_o(qr)$ is the zeroth order Bessel function of qr. The radial distribution function $2\pi r n(r)$ can be obtained by the Bessel transform

$$2\pi r n(r) = 2\pi r \bar{n} + r \iint [S(q) - 1] J_o(qr) q \, dq. \tag{3}$$

Experimentally measured $I(q)$ are not normalized, however. The procedure for deducing the radial distribution function from unnormalized $I(q)$ is described in Warren (1969) and He et al. (1993a).

First, we constructed the form factor from a molecular model based on the NMR structure; 250 frames of the gramicidin channel from a molecular dynamics simulation (Woolf and Roux, 1996) were used to obtain an average form factor (Fig. 7). It is interesting to note that this form factor is very close to the form factor of a cylindrical shell with 5.2 Å in inner diameter and 9.6 Å in outer diameter. These dimensions are close to the structural dimensions of the gramicidin backbone, indicating that the channel form factor is mainly that of the backbone. This is because only the rigid part of the molecule will contribute to the ensemble averaged form factor. The contribution of the side chains is for the most part motionally averaged to zero (for the lack of correlations). Next, the magnitude of the scattering intensity $I(q)$ was adjusted so its tail fit the square of the form factor: an example is shown in the inset of Fig. 8. $I(q)/|F(q)|^2$ is then the normalized structure factor $S(q)$. Finally, Eq. 3 is used to obtain the radial distribution function $2\pi r n(r)$ (Fig. 8). $2\pi r n(r)$ is a function that rises from near zero to a (local) maximum at the distance where there is a high probability for finding neighboring channels. This distance is the most probable nearest-neighbor separation between channels. Beyond this distance $2\pi r n(r)$ oscillates below and above the average density curve $2\pi r \bar{n}$.

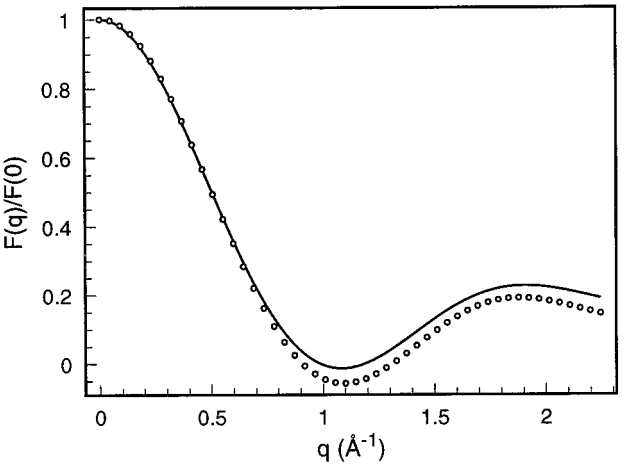

FIGURE 7 The normalized form factor of gramicidin channel. The solid line is the result of an ensemble average over 250 molecular configurations from a molecular dynamics simulation (Woolf and Roux, 1996). The circles are the form factor of a cylindrical shell with 5.2 Å in inner diameter and 9.6 Å in outer diameter, the structural dimensions of the gramicidin backbone.

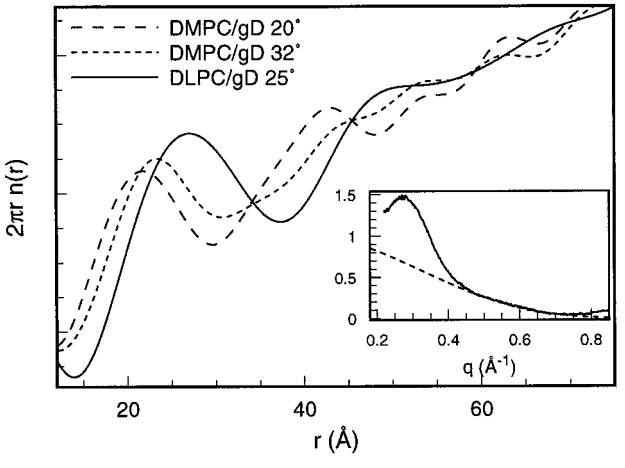

FIGURE 8 The inset shows that the scattering intensity $I(q)$ fits (by adjusting its overall magnitude) to the tail of the square of the normalized form factor (*dashed line*). The main frame shows unnormalized $2\pi r n(r)$. We are interested in the position of the first peak, which gives the most probable nearest-neighbor separation between gramicidin channels.

For the discussion of membrane-mediated interactions, we are interested in the nearest-neighbor separations in the fluid phase. From the first maxima in Fig. 8, we obtain the most probable nearest-neighbor separation 26.8 Å in DLPC and 23.3 Å in DMPC. Individual gramicidin channels diffuse randomly in the fluid phase, but in average the channels are 13% closer to each other in DMPC than in DLPC.

Although not the main subject of this paper, the distribution of gramicidin in the gel phase is also of interest (Killian, 1992; Mou et al., 1996). An atomic force spectroscopy (AFM) scan of gramicidin in the gel phase of DPPC (single bilayers supported on a mica surface) indicated cluster formations but could not resolve individual channels (Mou et al., 1996). In Fig. 5 we note that the gramicidin peak in the gel phase is sharper than in the fluid phase of DMPC. This indicates a higher probability of finding gramicidin-gramicidin separation at a well-defined separation in the gel phase than in the fluid phase. However, the absence of any higher-order peaks precludes the likelihood that gramicidin forms a lattice with a long-range order, consistent with the AFM result. From Fig. 8 we found the most probable nearest-neighbor separation to be 21.6 Å. For comparison, if the channels are uniformly distributed, the average separation between neighboring channels is 28.4 Å (assuming the area per lipid is 45 $Å^2$ and the area per channel is 250 $Å^2$). The diameter of the gramicidin channel is ~18 Å according to the NMR structure (Arseniev et al., 1985; Ketchem et al., 1993), 3.6 Å less than the most probable gramicidin-gramicidin separation. This indicates the aggregates could be a mixture of gramicidin and lipid.

CONCLUSION

We now concentrate on gramicidin in the fluid phase of DLPC and DMPC. The idea of hydrophobic matching is that one expects the thickness, h, of the hydrocarbon part of the membrane locally adjusts to the length, h_G, of the hydrophobic part of the channel. However, it is difficult to measure h and h_G directly. From the effect of membrane thickness on gramicidin channel lifetime, h_G was estimated to be ~22 Å (Elliott et al., 1983), substantially shorter than the physical length of the channel (~26 Å; Arseniev et al., 1985; Olah et al., 1991). Similarly, the definition for h has to be empirical. This is in part because the conformations of two lipid chains are not the same; the starting points of the two CH_2 chains are not at the same level. (The sn-1 chain is extended perpendicular to the bilayer surface at all CH_2 segments, whereas the sn-2 chain is bent, with the first CH_2 segment parallel and the rest of the chain perpendicular to the bilayer surface; Seelig and Seelig, 1980.) For clarity we denote h_o the thickness in pure lipid, h_b the thickness at the lipid-gramicidin boundary, and $\bar{h}$ the average thickness in a bilayer containing gramicidin. Hydrophobic matching implies $h_b = h_G$. However, $\bar{h}$ is in general different from h_b because the bilayer tends to restore itself to its unperturbed thickness h_o away from the boundary. Experimental evidence, including the results of x-ray crystallography (Hauser et al., 1981), deuterium NMR (Seelig and Seelig, 1980), neutron diffraction (Büldt et al., 1978), and x-ray diffraction (Chen, Hung, and Huang, in preparation) suggest that the glycerol region from the phosphate to the beginning of the hydrocarbon region is about the same in the gel and L_α phases (McIntosh and Simon, 1986; Nagle et al., 1996). This distance is ~5 Å (Nagle et al., 1996; Chen, Hung, and Huang, in preparation). Using this assumption, we estimate $\bar{h}$ ~PtP − 10 Å.

Interestingly, our data also support this relation between PtP and $\bar{h}$. DLPC containing gramicidin has a PtP = 32.1 Å. The above relation gives $\bar{h}$ = 22.1 Å essentially equal to the estimated h_G, as expected by hydrophobic matching. In this case $\bar{h} \sim h_b \sim h_G$ is reasonable, because the lipid's natural hydrocarbon thickness, h_o ~20.8 Å, is sufficiently close to h_G. For DMPC, h_o is sufficiently larger than h_G that we expect $\bar{h} > h_b \sim h_G$ as the measurement showed. The energy cost of hydrophobic matching is proportional to $(h_o - h_G)^2$ (Huang, 1986; 1995), so the strain energy in DLPC/gD is small compared with DMPC/gD. The strain field in the deformed bilayer creates an attractive membrane-mediated potential between gramicidin channels. This effect is also stronger in DMPC. As expected, we found the gramicidin-gramicidin distance in DMPC shorter than in DLPC. Thus our experiments confirm both the conjectures of hydrophobic matching and membrane-mediated interactions. In the next paper we will present a quantitative theory for these effects based on the deformation free energy previously used to explain the relation between membrane thickness and gramicidin channel lifetime (Huang, 1986).

We thank Benoit Roux for providing us with atomic coordinates of his molecular simulations.

This work was supported by NIH Grant GM55203 and NIH Training Grant GM08280, and by the Robert A. Welch Foundation.

REFERENCES

Abney, J. R., and J. C. Owicki. 1985. Theories of protein-lipid and protein-protein interactions in membranes. *In* Progress in Protein-Lipid Interactions. A. Watts and J. De Pont, editors. Elsevier Science Publishers, New York.

Arseniev, A. S., V. F. Bystrov, T. V. Ivanov, and Y. A. Ovchinnikov. 1985. ^{1}H-NMR study of gramicidin-A transmembrane ion channel. Head-to-head right-handed single stranded helices. *FEBS Lett.* 186: 168–174.

Beamer, L., S. F. Carroll, and D. Eisenberg. 1997. Crystal structure of human BPI and two bound phospholipids at 2.4 angstrom resolution. *Science.* 276:1757–1936.

Blasie, J. K., and C. R. Worthington. 1969. Planar liquid-like arrangement of photopigment molecules in frog retinal receptor disk membranes. *J. Mol. Biol.* 39:417–439.

Blaurock, A. E. 1971. Structure of the nerve myelin membrane: proof of the low resolution profile. *J. Mol. Biol.* 56:35–52.

Brown, M. F. 1997. Influence of nonlamellar-forming lipids on rhodopsin. *In* Current Topics in Membranes, vol. 44, Academic Press, New York. 285–356.

Büldt, G., H. U. Gally, A. Seelig, J. Seelig, and G. Zaccai. 1978. Neutron diffraction studies on selectively deuterated phospholipid bilayers. *Nature.* 271:182–184.

Caillé, A. 1972. Remarques sur la diffusion des rayons X dans les smectiques. *C. R. Acad. Sci. Serie B.* 274:891–893.

Chen, F. Y., W. C. Hung, and H. W. Huang. 1997. Critical swelling of phospholipid bilayers. *Phys. Rev. Lett.* 79:4026–4029.

Chothia, C. 1974. Hydrophobic bonding and accessible surface area in proteins. *Nature.* 248:338–339.

de Planque, M. R. R., D. V. Greathouse, R. E. Koeppe II, H. Schäfer, D. Marsh, and J. A. Killian. 1998. Influence of lipid/peptide hydrophobic mismatch on the thickness of diacylphosphatidylcholine bilayers: a ^{2}H-NMR and ESR study using designed transmembrane α-helical peptides and gramicidin A. *Biochemistry.* 37:9333–9345.

Elliott, J. R., D. Needham, J. P. Dilger, and D. A. Hayden. 1983. The effects of bilayer thickness and tension on gramicidin single-channel lifetime. *Biochim. Biophys. Acta.* 735:95–103.

Evans, E. A., and D. Needham. 1987. Physical properties of surfactant bilayer membranes: thermal transitions, elasticity, rigidity, cohesion, and colloidal interactions. *J. Phys. Chem.* 91:4219–4228.

Gekko, K., and H. Noguchi. 1979. Compressibility of globular proteins in water at 25°C. *J. Phys. Chem.* 83:2706–2714.

Goulian, M. 1996. Inclusions in membranes. *Curr. Opin. Colloid Interface Sci.* 1:358–361.

Hauser, H., I. Pascher, R. H. Pearson, and S. Sundell. 1981. Preferred conformation and molecular packing of phosphatidylethanolamine and phosphatidylcholine. *Biochim. Biophys. Acta.* 650:21–51.

He, K., S. J. Ludtke, W. T. Heller, and H. W. Huang. 1996b. Mechanism of alamethicin insertion into lipid bilayers. *Biophys. J.* 71:2669–2679.

He, K., S. J. Ludtke, D. L. Worcester, and H. W. Huang. 1995. Antimicrobial peptide pores in membranes detected by neutron in-plane scattering. *Biochemistry.* 34:15614–15618.

He, K., S. J. Ludtke, D. L. Worcester, and H. W. Huang. 1996a. Neutron scattering in the plane of membrane: structure of alamethicin pores. *Biophys. J.* 70:2659–2666.

He, K., S. J. Ludtke, Y. Wu, and H. W. Huang. 1993a. X-ray scattering with momentum transfer in the plane of membrane: application to gramicidin organization. *Biophys. J.* 64:157–162.

He, K., S. J. Ludtke, Y. Wu, and H. W. Huang. 1993b. X-ray scattering in the plane of membrane. *J. Phys. France IV.* 3:265–270.

He, K., S. J. Ludtke, Y. Wu, H. W. Huang, O. S. Andersen, D. Greathouse, and R. E. Koeppe. 1994. Closed state of gramicidin channel detected by x-ray in-plane scattering. *Biophys. Chem.* 49:83–89.

Hinton, J. F., J. Q. Fernandez, D. C. Shungu, W. L. Whaley, R. E. Koeppe, and F. S. Millett. 1988. T1–205 nuclear magnetic resonance determination of the thermodynamic parameters for the binding of monovalent cations to gramicidins A and C. *Biophys. J.* 54:527–533.

Huang, H. W. 1986. Deformation free energy of bilayer membrane and its effect on gramicidin channel lifetime. *Biophys. J.* 50:1061–1070.

Huang, H. W. 1995. Elasticity of lipid bilayer interacting with amphiphilic helical peptides. *J. Phys. France II.* 5:1427–1431.

Huang, H. W., and G. A. Olah. 1987. Uniformly oriented gramicidin channels embedded in thick monodomain lecithin multilayers. *Biophys. J.* 51:989–992.

Ketchem, R. R., W. Hu, and T. A. Cross. 1993. High-resolution conformation of gramicidin A in a lipid bilayer by solid-state NMR. *Science.* 261:1457–1460.

Killian, J. A. 1992. Gramicidin and gramicidin-lipid interactions. *Biochim. Biophys. Acta.* 1113:391–425.

Koeppe II, R. E., T. C. B. Vogt, D. V. Greathouse, J. A. Killian, and B. De Kruijff. 1996. Conformation of the acylation site of palmitoylgramicidin in lipid bilayers of dimyristoylphosphatidylcholine. *Biochemistry.* 35: 3641–3648.

Lewis, B. A., and D. M. Engelman. 1983. Bacteriorhodopsin remains dispersed in fluid phospholipid bilayers over a wide range of bilayer thickness. *J. Mol. Biol.* 166:203–210.

Loewenstein, W. R. 1981. Junctional intercellular communications: the cell to cell membrane channel. *Physiol. Rev.* 61:829–913.

Ludtke, S., K. He, and H. W. Huang. 1995. Membrane thinning caused by magainin 2. *Biochemistry.* 34:16764–16769.

Luzzati, V. 1968. X-ray diffraction studies of lipid-water systems. *In* Biological Membranes. D. Chapman, editor. Academic Press, New York. 71–124.

Marcelja, S. 1976. Lipid-mediated protein interaction in membranes. *Biochim. Biophys. Acta.* 455:1–7.

McIntosh, T. J., and S. A. Simon. 1986. Area per molecule and distribution of water in fully hydrated dilauroylphosphatidylethanolamine bilayers. *Biochemistry.* 25:4948–4952.

Morrow, M. R., and J. H. Davis. 1988. Differential scanning calorimetry and ^{2}H NMR studies of the phase behavior of gramicidin-phosphatidylcholine mixtures. *Biochemistry.* 27:2024–2032.

Mou, J., D. M. Czajkowsky, and Z. Shao. 1996. Gramicidin A aggregation in supported gel state phosphatidylcholine bilayers. *Biochemistry.* 35: 3222–3226.

Nagle, J. F., R. Zhang, S. Tristram-Nagle, W. Sun, H. I. Petrache, and R. M. Suter. 1996. X-ray structure determination of fully hydrated L_α phase dipalmitoylphosphatidylcholine bilayers. *Biophys. J.* 70: 1419–1431.

Olah, G. A. 1990. TL^+ distribution in the gramicidin ion conducting channel determined by X-ray diffraction. Ph.D. Thesis, Rice University, Houston, TX.

Olah, G. A., H. W. Huang, W. Liu, and Y. Wu. 1991. Location of ion binding sites in the gramicidin channel by x-ray diffraction. *J. Mol. Biol.* 218:847–858.

Owicki, J. C., and H. M. McConnell. 1979. Theory of protein-lipid and protein-protein interactions in bilayer membranes. *Proc. Natl. Acad. Sci. USA.* 76:4750–4754.

Pearson, L. T., S. I. Chan, B. A. Lewis, and D. M. Engelman. 1983. Pair distribution functions of bacteriorhodopsin and rhodopsin in model bilayers. *Biophys. J.* 43:167–174.

Pearson, L. T., J. Edelman, and S. I. Chan. 1984. Statistical mechanics of lipid membranes. Protein correlation functions and lipid ordering. *Biophys. J.* 45:863–871.

Phillips, W. C., and G. N. Phillips, Jr. 1985. Two new x-ray films: conditions for optimum development and calibration of response. *J. Appl. Crystallogr.* 18:3–7.

Rokitskaya, T. I., Y. N. Antonenko, and E. A. Kotova. 1996. Photodynamic inactivation of gramicidin channels: a flash-photolysis study. *Biochim. Biophys. Acta.* 1275:116–221.

Schindler, H., and J. Seelig. 1975. Deuterium order parameters in relation to thermodynamic properties of a phospholipid bilayer: a statistical mechanical interpretation. *Biochemistry.* 14:2283–2287.

Schroeder, H. 1977. Aggregation of proteins in membranes: an example of fluctuation-induced interactions in liquid crystals. *J. Chem. Phys.* 67: 1617–1619.

Seelig, J., and A. Seelig. 1980. Lipid conformation in model membranes and biological membranes. *Q. Rev. Biophys.* 13:19–61.

Smith, G. S., E. B. Sirota, C. R. Safinya, R. J. Plano, and N. A. Clark. 1990. X-ray structural studies of freely suspended ordered hydrated DMPC multimembrane films. *J. Chem. Phys.* 92:4519–4529.

Stoeckenius, W., R. H. Lozier, and R. A. Bogomolni. 1979. Bacteriorhodopsin and the purple membrane of halobacteria. *Biochim. Biophys. Acta.* 505:215–278.

Urry, D. W., A. Spisni, and M. A. Khaled. 1979a. Characterization of micellar-packaged gramicidin A channels. *Biochem. Biophys. Res. Commun.* 88:940–949.

Urry, D. W., A. Spisni, M. A. Khaled, M. M. Ling, and L. Masotti. 1979b. Transmembrane channels and their characterization in phospholipid structures. *Int. J. Quantum Chem. Quantum Biol.* 6:289–303.

Warren, B. E. 1969. X-ray Diffraction. Dover Publications, Mineola, New York. 116–150.

Woolf, T. B., and B. Roux. 1996. Structure, energetics, and dynamics of lipid-protein interactions: a molecular dynamics study of the gramicidin A channel in a DMPC bilayer. *Proteins.* 24:92–114.

Wu, Y., K. He, S. J. Ludtke, and H. W. Huang. 1995. X-ray diffraction study of lipid bilayer membrane interacting with amphiphilic helical peptides: diphytanoyl phosphatidylcholine with alamethicin at low concentrations. *Biophys. J.* 68:2361–2369.

Wu, Y., H. W. Huang, and G. A. Olah. 1990. Method of oriented circular dichroism. *Biophys. J.* 57:797–806.